Quantum Electronics **35** (6) 495 – 503 (2005)

LASERS

PACS numbers: 42.55.Ks; 42.60.By; 42.60.Lh
DOI: 10.1070/QE2005v035n06ABEH002866

Highly efficient cw chemical oxygen – iodine laser with transsonic iodine injection and a nitrogen buffer gas

A.S. Boreisho, A.B. Barkan, D.N. Vasil'ev,
I.M. Evdokimov, A.V. Savin

***Abstract*. Methods of increasing the efficiency of low-pressure chemical oxygen – iodine lasers (COILs) with transsonic injection of molecular iodine, in which nitrogen is used as a buffer gas, are studied. A two-layer gas-dynamic model is used for a parametric analysis of physicochemical processes occurring in the transsonic iodine injector and in the COIL resonator, including mixing and generation of radiation. The 3D-RANS computer simulation software is used to study the flow structures resulting from an injection of iodine-containing flow into the transsonic zone of the oxygen nozzle. Experiments with a 10-kW modified laser have resulted in a chemical efficiency of 31.5 % for a lasing power of 13.5 kW. The results of experimental studies of the cryosorption COIL exhaust system are presented.**

Keywords: *oxygen – iodine laser, singlet oxygen, chemical efficiency, gain, 3D-RANS simulation software.*

1. Introduction

A cw chemical oxygen – iodine laser (COIL) is the most attractive source of laser radiation for a whole range of applications. A short wavelength and a high optical quality of the laser medium make it indispensable in cases where the laser radiation energy must be transported over large distances with minimum losses. Research on COILs, which has been going on for over a quarter of a century, is currently aimed at increasing the efficiency of such lasers since the fundamental problems of their physics and technology have already been solved. One of the most important and not completely exhausted resources for enhancing the COIL efficiency concerns the modification of the gas-dynamic processes responsible for the formation of the active medium.

For example, one of the important limiting factors determining the COIL efficiency is the singlet oxygen loss during the dissociation of molecular iodine. At the first stage, the direct dissociation of the iodine molecule $I_2 + O_2(^1\Sigma) \rightarrow 2I + O_2(^1\Delta)$ plays the fundamental role. This stage proceeds quite slowly since the concentration of sigma oxygen is quite low and the rate constant of the reaction is also small. After the concentration of iodine atoms becomes significant, the second (more rapid) dissociation stage sets in, when the iodine atoms play the role of the transport channel during transfer of energy to molecular iodine

$$\begin{aligned} &I + O_2(^1\Delta) \rightarrow I^* + O_2(^3\Sigma), \\ &I^* + I_2 \rightarrow I + I_2^*, \\ &I_2^* + O_2(^1\Delta) \rightarrow 2I + O_2(^3\Sigma). \end{aligned} \qquad (1)$$

Traditionally, it is assumed that about 5 – 6 singlet oxygen molecules are spent on each iodine molecule during dissociation of molecular iodine, while according to the scheme (1), the rapid stage requires just two molecules of singlet oxygen. The remaining losses occur due to two reasons. First, before a complete mixing of oxygen and iodine flows, there exist regions with a high local concentration of molecular iodine in which singlet oxygen is completely quenched, e.g., according to the scheme

$$\begin{aligned} &O_2(^1\Delta) + I \rightarrow O_2(^3\Sigma) + I^*, \quad k = 7.7 \times 10^{-11}\ \mathrm{cm^3\ s^{-1}}, \\ &I^* + I_2 \rightarrow I_2^* + I, \quad k = 3.5 \times 10^{-11}\ \mathrm{cm^3\ s^{-1}}, \\ &I_2^* + N_2 \rightarrow I_2 + N_2, \quad k = 9 \times 10^{-12}\ \mathrm{cm^3\ s^{-1}}. \end{aligned} \qquad (2)$$

Second, water vapour, which is always present in the active medium of a laser with a chemical singlet oxygen generator, actively facilitates the quenching of excited iodine atoms, and an additional active quenching channel

$$\begin{aligned} &I + O_2(^1\Delta) \rightarrow I^* + O_2(^3\Sigma), \\ &I^* + H_2O \rightarrow I + H_2O \end{aligned} \qquad (3)$$

is operative as long as singlet oxygen remains in the flow. Hence, the faster the mixing of oxygen and iodine flows, the lower the loss of singlet oxygen and hence the higher the

A.S. Boreisho, A.B. Barkan, D.N. Vasil'ev, I.M. Evdokimov, A.V. Savin
D.F. Ustinov Voenmekh Baltic State Technical University,
Laser Systems Ltd., 1-ya Krasnoarmeiskaya ul. 1, 190005 St. Petersburg, Russia; e-mail: savin@lsystems.ru; website: www.lsystems.ru

Received 16 September 2004; revision received 22 March 2005
Kvantovaya Elektronika **35** (6) 495 – 503 (2005)
Translated by Ram Wadhwa

COIL efficiency. This is the reason behind the considerable attention being paid to the problems of mixing during the preparation of the active medium. However, the gas-dynamic expansion required for attaining a high gain and suppression of quenching in channel (3) hampers the mixing of flows and thus increases the losses in channel (2). Hence, it is necessary to obtain a correct synchronisation of the mixing and expansion processes.

If helium is used as the buffer gas, the velocity of the active medium is quite high, the time required for transporting the medium from the reaction zone to the nozzle bank is small and hence the losses are comparatively low. However, the use of helium lowers the effective molecular weight of the active medium to 9–10 atomic units. The exhaust of such an active medium requires an enormous energy expenditure and hence lowers the efficiency of the laser system as a whole [1]. The quenching problems become quite significant in the case when nitrogen is used as the buffer gas instead of helium since the active medium velocity becomes much lower in this case and accordingly the medium transportation time becomes longer. Nevertheless, an enhanced efficiency of the exhaust systems renders nitrogen-based COILs much more effective.

In this article, we study the methods of increasing the efficiency of low-pressure oxygen–iodine lasers [2] with transsonic injection of molecular iodine and with nitrogen as buffer gas. A two-layer gas-dynamic model [3] is used for a parametric analysis of physicochemical processes occurring in the transsonic iodine injector and in the COIL resonator, including mixing and generation of radiation. The 3D-RANS computer simulation software [4] is used to study the flow structures resulting from an injection of iodine-containing flow into the transsonic zone of the oxygen nozzle. Experiments with a 10-kW modified laser [2] have resulted in a chemical efficiency of 31.5 % for a lasing power of about 14 kW. The results of experimental studies of the cryosorption COIL exhaust system are presented.

2. Computer simulation of the gas-dynamic processes occurring in the active medium of COILs

The specification of conditions imposed on the mixing process based on the final laser parameters requires a simplified gas-dynamic model of the active medium, suitable for a wide-range parametric computer experiment for simulating the transformation of the active medium energy into laser energy in situations characteristic of the nozzle banks of COILs. Such a model must describe the kinetic processes, gas-dynamic cooling, and mixing. In familiar models of this kind [5], an attempt is made at describing mechanical mixing also in the same manner. Since a rigorous description is impossible, certain *a priori* concepts about the mixing mechanism have to be introduced in the model, which makes the obtained results less objective. At present, when highly effective means have been developed for three-dimensional simulation of flows with a complex physics and chemistry, it is possible to solve two problems independently: (i) the conditions imposed on the mixing process can be determined using simplified models, after which (ii) the three-dimensional mechanism of mixing is studied and the ways of achieving the required values of parameters are found.

2.1 Simulation of kinetics and mixing using a two-layer gas-dynamic model of the active medium

To solve the first of the above-mentioned problems, a two-layer gas-dynamic model was developed to describe the flow in the nozzle bank and the resonator of a COIL [3]. The simplest flow scheme used for constructing a mixing model consists of the two layers being mixed. Each layer is described by one-dimensional gas-dynamic equations, and the mixing is simulated by the source terms on the right-hand side of the transport equations. It is assumed that pressure is a function of longitudinal coordinate and is identical for both layers. Under such a formulation, the mixing rate is treated as an external parameter.

The equations of motion for each layer contain the action of the pressure forces and momentum exchange between the layers:

$$\mu_1 c_1 u_1 \frac{\mathrm{d}u_1}{\mathrm{d}x} = -\frac{\mathrm{d}p}{\mathrm{d}x} + m\mu_2 c_2 \frac{1-A}{A}(u_2 - u_1), \tag{4}$$

$$\mu_2 c_2 u_2 \frac{\mathrm{d}u_2}{\mathrm{d}x} = -\frac{\mathrm{d}p}{\mathrm{d}x} + m\mu_1 c_1 \frac{A}{1-A}(u_1 - u_2), \tag{5}$$

where the subscripts 1 and 2 indicate parameters of the first and second layer, respectively; p is the pressure having the same value for both layers; u is the velocity; μ is the molecular weight; c is the molar density; A is the fraction of the cross-sectional area occupied by the first layer; and m is the mixing rate parameter.

The equation of mass conservation contains chemical transformations and mass exchange between the layers:

$$\frac{\mathrm{d}c_{i1}}{\mathrm{d}x} = -c_{i1}\left(\frac{\mathrm{d}u_1}{u_1\mathrm{d}x} + \frac{\mathrm{d}F}{F\mathrm{d}x} + \frac{\mathrm{d}A}{A\mathrm{d}x}\right)$$

$$+\frac{1}{u_1}\sum_{j=1}^{n_\mathrm{r}} k_j(\nu''_{ji} - \nu'_{ji})\prod_{k=1}^{n_\mathrm{c}} c_{k_1}^{\nu'_{jk}} + \frac{m}{u_1}\left(\frac{1-A}{A}c_{i2} - c_{i1}\right), \tag{6}$$

$$\frac{\mathrm{d}c_{i2}}{\mathrm{d}x} = -c_{i2}\left[\frac{\mathrm{d}u_2}{u_2\mathrm{d}x} + \frac{\mathrm{d}F}{F\mathrm{d}x} - \frac{\mathrm{d}A}{(1-A)\mathrm{d}x}\right]$$

$$+\frac{1}{u_2}\sum_{j=1}^{n_\mathrm{r}} k_j(\nu''_{ji} - \nu'_{ji})\prod_{k=1}^{n_\mathrm{c}} c_{k_2}^{\nu'_{jk}} + \frac{m}{u_2}\left(\frac{A}{1-A}c_{i1} - c_{i2}\right), \tag{7}$$

where c_{ij} is the molar density of the jth component of the mixture in the ith layer; F is the variable area of cross section of the channel in which the reactive flow being mixed moves; ν are the stoichiometric reaction coefficients (the subscripts indicate the reaction number and the mixture component number, while the single and double primes mark the left and right stoichiometric reaction coefficients, respectively); k_j is the rate constant of the jth reaction (in $\mathrm{m^3\ mole^{-1}\ s^{-1}}$); and n_r and n_c are, respectively, the number of reactions and components in the mixture.

The first term in the right-hand side of Eqns (6), (7) is of purely gas-dynamic origin and corresponds to the so-called impact reversal equation [6], the second term describes chemical transformations [7] and the third term describes the mass exchange between the layers. In the absence of chemical reactions and exchange between the layers, the equations are transformed into classical one-dimensional gas-dynamic equations. All the equations are completely symmetric to transposition of layers.

The energy equations for both layers have the form

$$\frac{\mathrm{d}}{\mathrm{d}x}\left(h_\mathrm{m}+\frac{u^2}{2}\right)_1=\frac{m}{u_1}\frac{\rho_1}{\rho_2}\frac{1-A}{A}\left[\left(h_\mathrm{m}+\frac{u^2}{2}\right)_2-\left(h_\mathrm{m}+\frac{u^2}{2}\right)_1\right]$$

$$-\delta(x)\frac{\sigma J}{u_1}\left(\left[\mathrm{I}^*\right]-\frac{1}{2}\left[\mathrm{I}\right]\right)_1\left(\frac{RT}{\mu p}\right)_1, \qquad (8)$$

$$\frac{\mathrm{d}}{\mathrm{d}x}\left(h_\mathrm{m}+\frac{u^2}{2}\right)_2=\frac{m}{u_2}\frac{\rho_1}{\rho_2}\frac{A}{1-A}\left[\left(h_\mathrm{m}+\frac{u^2}{2}\right)_1-\left(h_\mathrm{m}+\frac{u^2}{2}\right)_2\right]$$

$$-\delta(x)\frac{\sigma J}{u_2}\left(\left[\mathrm{I}^*\right]-\frac{1}{2}\left[\mathrm{I}\right]\right)_2\left(\frac{RT}{\mu p}\right)_2, \qquad (9)$$

where [I*] and [I] are the atomic iodine concentrations in the excited and unexcited states, respectively; h_m is the enthalpy of a unit mass including the enthalpy of its formation; $\delta(x)$ is a function equal to unity in the cavity and zero outside it; J is the intracavity field intensity; and σ is the induced emission cross section. The intracavity field intensity is assumed to be constant in time and in space within the cavity volume, which is close to reality under conditions of a multimode stable cavity.

The analysis of the energy flux balance at the output mirror allows us to compute the output power of a COIL if the intracavity intensity J is known:

$$P_\mathrm{out}=\frac{\tau}{2-(\tau+\beta)}JS, \qquad (10)$$

where S is the area of the output aperture; β is the nonresonant loss coefficient; and τ is the transmission coefficient (transparency) of the output mirror. Under the intracavity field conditions, the gain of the medium is defined as

$$g=\sigma\Delta N=\sigma\left(\left[\mathrm{I}^*\right]-\frac{1}{2}\left[\mathrm{I}\right]\right),$$

where ΔN is the inversion of the active medium. The steady state condition for the radiant energy density in the cavity volume leads to the following expression for the transmission coefficient of the output mirror:

$$\tau=(2-\beta)\left\{1+\frac{S}{\sigma}\left[\int_0^L F(x)\sigma\left(\left[\mathrm{I}^*\right]-\frac{1}{2}\left[\mathrm{I}\right]\right)\mathrm{d}x\right]^{-1}\right\}^{-1}. \qquad (11)$$

Thus, if the external mixing rate parameter m is known, the two-layer gas-dynamic model (4)–(9) can be used to solve the gas-dynamic problem on the motion of reactive flow being mixed in a channel of a variable cross section under lasing conditions. In this case, the intracavity field intensity is also defined as a parameter after which the transmission coefficient of the output mirror corresponding to the obtained solution is calculated using relation (11).

Consider the conditions characteristic of a 10-kW laser [2]. Singlet oxygen is produced as a result of interaction of gaseous chlorine with basic hydrogen peroxide, and the flow rate of chlorine is the main dimensional parameter determining the lasing power. The length of the active medium along the optical axis of the resonator is $B=37$ cm, the aperture size is 6×6 cm, the nozzle expansion ratio is 2 : 1, the oxygen flow pressure in front of the nozzle is 25 Torr, the primary dilution (ratio of molar flow rate of primary nitrogen to the molar flow rate of chlorine) $D_1=2$, the titration ratio (ratio of molar flow rate of molecular iodine to the molar flow rate of chlorine) is 4 %, the secondary dilution $D_2=1$, the relative concentration of water vapour in the primary flow is $w=0.1$, the chlorine utilization $\mathrm{Ut}=0.95$, and the yield of singlet oxygen is $Y=0.6$. The initial conditions are specified for the critical nozzle cross section, and the transsonic mixing scheme is used.

Figure 1a shows the dependence of the output power on the mixing rate parameter m and transmission coefficient τ of the output mirror. The nonresonant loss coefficient β was assumed to be equal to 0.01. For the 10-kW laser considered in this work, the quantity β does not have a strong influence on the results, since β is usually much smaller than τ. Calculations show that if the resonator begins directly from the nozzle edge, an increase in the mixing rate leads to a monotonic increase in the lasing power. For $m\approx10^4$ s^{-1} and $\tau=0.05-0.07$, the lasing power is about 12 kW. This is in accord with the experimental results [2]. The threshold transparency increases with the mixing rate, tending to the value $\tau\approx0.25$.

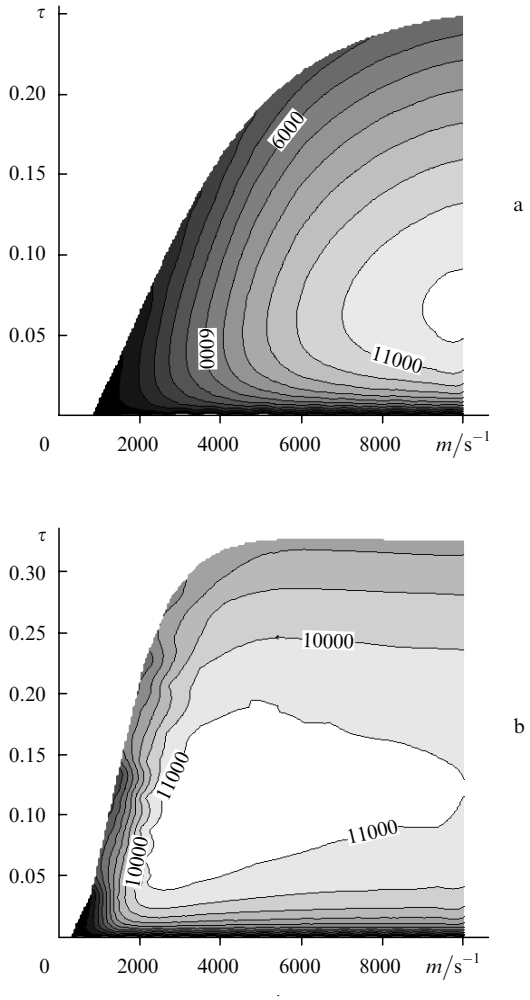

Figure 1. Dependence of the output power on the mixing rate parameter m and the the transmission coefficient τ of the mirrors for the case when the resonator cavity begins from the nozzle edge (a) and when the cavity is displaced by 6 cm (b); the numbers on the level lines indicate the power in watts.

Figure 1b shows the results of parametric analysis for the case when the resonator is displaced downstream from the nozzle edge by 6 cm. One can see that the maximum power has virtually remained unchanged, but an optimal value of the mixing rate is attained. This is associated with the energy loss mechanism. The main loss channel is connected with the quenching of excited iodine atoms by water molecules, hence the higher the dissociation rate, the higher the losses leading to heating of the medium. If the resonator is displaced downstream, a high mixing rate may even be harmful since it causes a too early dissociation and additional losses in channel (3).

This means that an optimal position of the resonator relative to the nozzle must be chosen for each nozzle design determining the mixing rate. A downstream displacement of the resonator causes a decrease in the optimal mixing rate, a decrease in the sensitivity to its variation, and an increase in the threshold transparency. The output laser power becomes less sensitive to variations in the design and operational parameters. For example, for an optimal mixing rate $m \approx 4000\ \mathrm{s}^{-1}$ in the situation depicted in Fig. 1b, the laser works at a power level of over 11 kW in the transparency window 0.04 – 0.18 of the mirror.

2.2 Analysis of vortex structures emerging during transsonic blowing of secondary flow

In order to analyse the mixing mechanism and the ways of attaining the required mixing rate for transsonic scheme of iodine supply, we calculated the flows in nozzles with injecting holes of various configurations.

The three-dimensional nonstationary Navier – Stokes equations were solved in the computational volume formed by the symmetry element of the nozzle system of the COIL (Fig. 2). Calculations were made by using the VICON-C [4] and CFX-5.5 software. To describe the chemical processes occurring in the gaseous phase, we used the kinetic scheme incorporating 34 reactions and 12 components of the gaseous mixture [2]. Together with the model of laminar flow of a thermodynamically ideal gas mixture, such a kinetic scheme has been used as a well-tested instrument for computer simulation of the gas-dynamics of the active medium of the COIL [10].

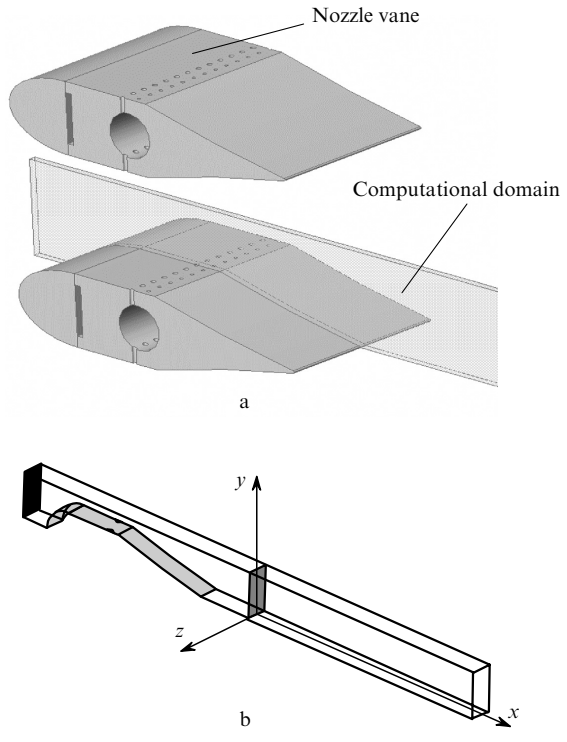

Figure 2. Position of the computational domain in the nozzle slit (a) and its schematic representation (b).

We considered three schemes of transsonic injection of secondary flow: a single row injector, a double-row injector with a continuous in-line arrangement of holes, and a double-row injector with a staggered arrangement of holes. The results of calculation of the penetration depth h of secondary flow streams into the primary flow are shown in Fig. 3 for various types of injectors. The same figure also shows the generalising dependence for a solitary stream injected into an unbounded entraining stream [9]. For a two-row injector, the penetration depth differs from the ideal value due to the interaction of flows from different rows of the injector. This effect lowers the flow mixing efficiency in the nozzle and hence leads to a nonequilibrium concentration distribution of components in the resonator resulting eventually in a nonequilibrium concentration distribution of components in the resonator (Fig. 4).

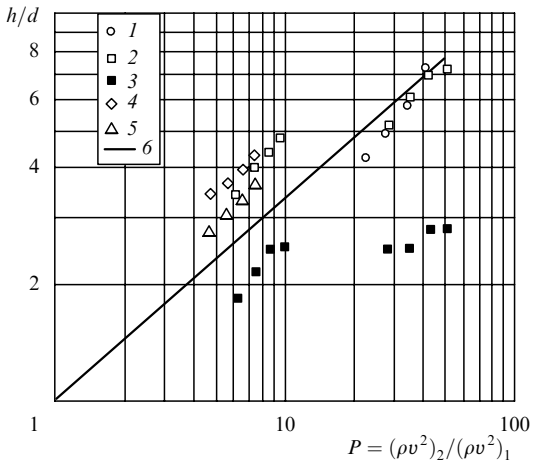

Figure 3. Dependence of the normalised penetration depth h for the streams being injected into the entraining flow on the ratio of the secondary (iodine) flow strength $(\rho v^2)_2$ to the primary (oxygen) flow strength $(\rho v^2)_1$ in the case of a one-row injector (*1*), two-row injector with a staggered arrangement of holes (*2*, *3* correspond to the first and second row, respectively), and a double-row injector with a continuous in-line arrangement of holes (*4*, *5* correspond to the first and second row, respectively); the straight line (*6*) describes the penetration depth for a solitary stream [8] (d is the injector hole diameter).

Consider in detail the mechanism of mixing in the nozzle channel of a 10-kW laser [2]. The transsonic iodine injector has two rows of holes arranged in staggered order.

Figure 5 shows the dependence of the iodine concentration dispersion D_1 (number of iodine atoms per unit volume in the diatomic molecule as well as in the dissociated state) normalised along x and z axes, on the coordinate x along the flow; $x = -30$ mm corresponds to the point of iodine injection, $x = 0$ corresponds to the nozzle exit. The concentration dispersion (standard deviation from the average value) is used as a measure characterising the nonuniformity of iodine distribution in any direction. The process

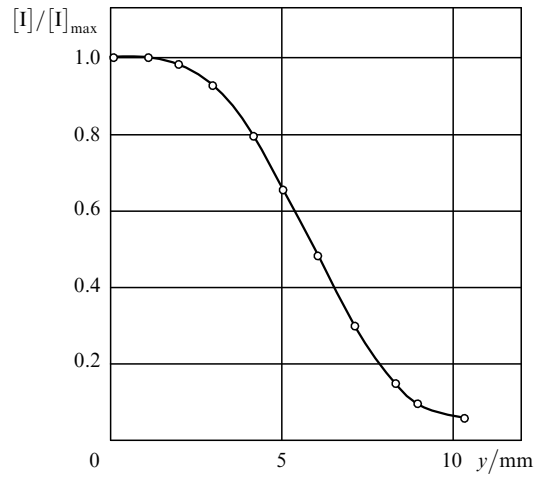

Figure 4. Relative iodine concentration distribution along the y axis at the nozzle exit, $[I]_{max}$ is the maximum iodine concentration in the given section.

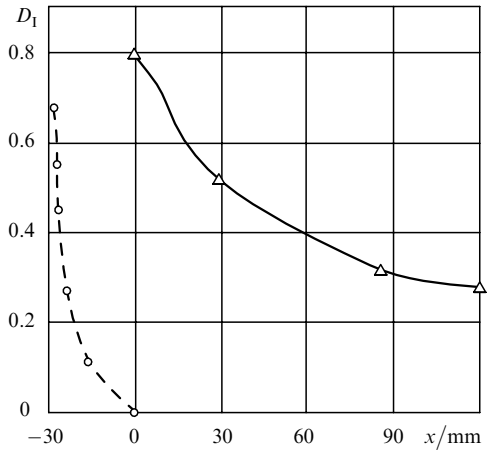

Figure 5. Distribution of normalised dispersion D_1 of the concentration of iodine atoms along the flow for the injector described in [2] for the case of dispersion along the y (solid curve) and z (dashed curve) axes for a stagnation pressure $p_{0(2)} = 88$ Torr of the secondary flow.

of mixing along the y axis (at a normalised dispersion level of 0.15) does not terminate even at a distance of 120 mm from the the nozzle exit. This leads to an unfinished dissociation and nonequilibrium generation of singlet oxygen. The concentrations level out much more rapidly along the z axis and the mixing process is completed near the nozzle exit since the scale of nonuniformities is much smaller. The mixing length along this axis is $L_m \approx 7.5$ mm, which corresponds to about 10–11 diameters of the injector holes in the first row.

Experiments aimed at studying the injection of a circular stream in an entraining flow reveal [2] that the stream being injected assumes a horse-shoe shape with two vortices. A similar effect is also observed during transsonic injection of iodine. For a small secondary flow rate and hence a small penetration depth parameter, 'underpenetration' of the stream is observed and a nonequilibrium iodine concentration is preserved in the entire computational domain (Fig. 6b).

Indeed, the first row stream forms a classical horse-shoe pattern (frame 2) corresponding to a pair of longitudinal vortices. The flow field of such a vortex pair disrupts the streams in the second row (frames 4 and 5). Two isolated vortex filaments are formed from the second row stream instead of a horse-shoe structure, their movement completely following the vortex field of the first stream (frames 6). This leads to the formation of a unified structure which looks like a localised region of high iodine concentration after attenuation of the vortex flow. Due to the interaction between the streams, a uniformity of concentrations cannot be provided even by increasing the penetration parameter.

An analysis of the mixing mechanism and three-dimensional structure of flows formed upon transsonic injection of the secondary flow leads to the formulation of a number of requirements which must be satisfied during the development of efficient mixing schemes in a COIL. The main requirements are as follows:

(i) The vortex structure must cover the entire cross section of the flow. Interaction between the injected streams must not lead to the formation of localised structures.

(ii) The characteristic molecular diffusion times must match the times of movement of vortex structures, as well as

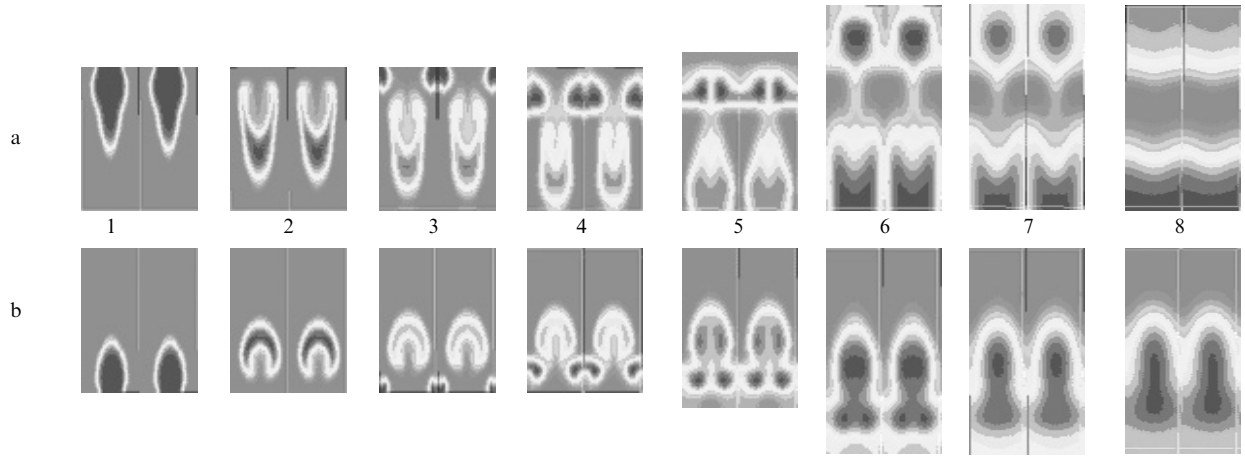

Figure 6. Sequential arrangement of frames with the water vapour concentration distribution over the nozzle cross sections under a secondary flow pressure $p_{0(2)} = 160$ Torr (a) and $p_{0(2)} = 88$ Torr (b) in front of the injector: (1) blowing through the first row holes, (3) blowing through the second row holes, (5–7) supersonic expansion, (8) supersonic flow region at a distance of 60 mm from the nozzle exit.

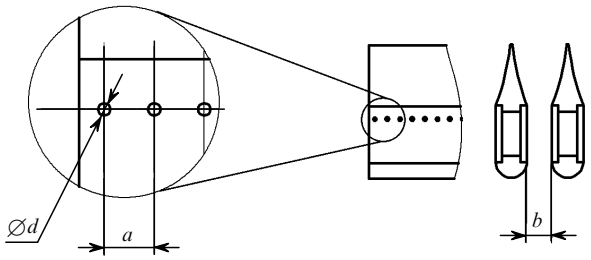

Figure 7. Scheme of a modernised transsonic iodine injector (two projections of the nozzle blade are shown).

the times of longitudinal convection of the active medium from the point of injection to the resonator.

The modernised gas-dynamic scheme of a transsonic secondary flow injector developed in accordance with these requirements contains one row of holes (Fig. 7).

Figure 8 shows a series of transverse flow cross sections of the active medium, starting from the point of injection of iodine. The vortex structure is formed in such a way that a sequence of plane layers separated by a distance equal to the spacing between the injector holes is formed near the nozzle exit. Subsequent levelling out of concentrations occurs because of molecular diffusion. Thus, the mixing process can be divided into two stages. At the first stage, concentration equalisation takes place along the direction of injection at scales of the order of transverse cross-section of the oxygen nozzle. This process is associated with the formation of vortex structures and is mainly of nonviscous origin. Its characteristic time can be estimated as $\tau_1 \approx b/(2u_{ef})$, where b is the transverse size of the nozzle and u_{ef} is the effective transverse velocity of the streams being injected. The second stage is mainly associated with diffusion and its characteristic time τ_2 is proportional to $(\frac{1}{2}a)^2/\nu$, where a is the spacing between the injector holes and ν is the kinematic viscosity. The proportions and absolute size of the nozzle apparatus are chosen in such a way that these characteristic times match with one another and with the convective time $\tau_c \approx L/u_{ch}$, where u_{ch} is the characteristic velocity of longitudinal motion of the medium being injected.

Figure 9 shows the distribution of the reduced y-dispersion D_1 of the concentration of iodine atoms in the direction of the flow. At a distance of 15 mm from the nozzle edge, the reduced dispersion becomes less than 15 % while at a distance of 40 mm it falls below 5 %. This leads to the formation of a homogeneous active medium with a high

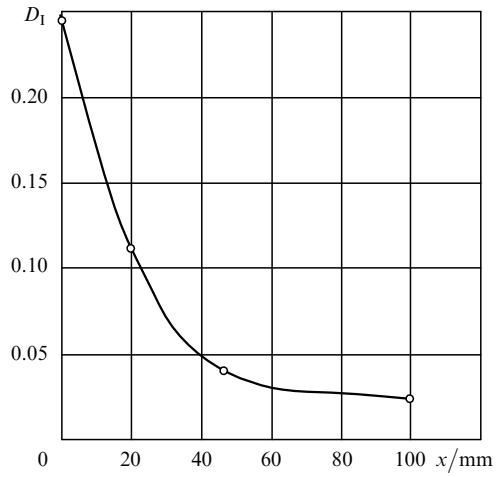

Figure 9. Distribution of the reduced dispersion D_1 (along the y axis) of the concentration of iodine atoms along the flow for the modernised mixing scheme ($x = 0$ corresponds to the nozzle exit), $p_{0(2)} = 256$ Torr.

gain. Figure 10 shows the distribution of the small-signal gain K_g averaged along the optical axis of the resonator for two types of transsonic injectors. One can see that the modified injector creates an active medium with a much higher gain.

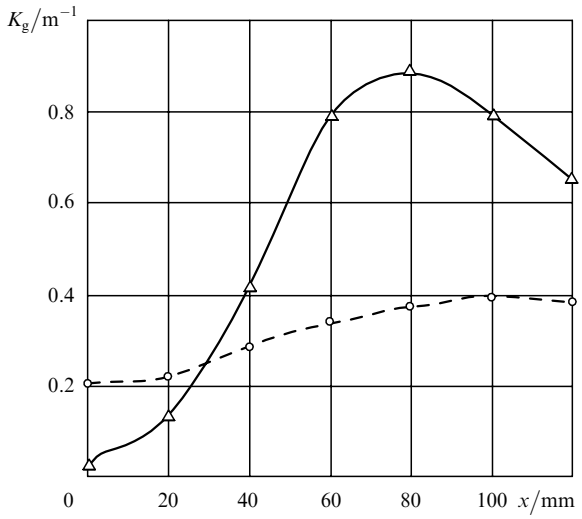

Figure 10. Averaged gain distribution for a small-signal gain in a modernised injector (solid curve) and the injector described in [2] (dashed curve).

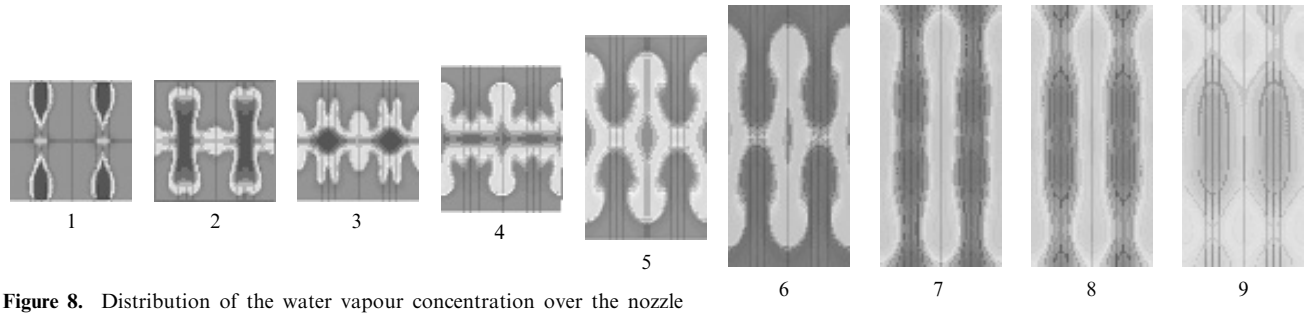

Figure 8. Distribution of the water vapour concentration over the nozzle cross sections of a modernised iodine injector for pressure $p_{0(2)} = 256$ Torr: (1) blowing; (4–6) supersonic expansion; (9) supersonic flow region at a distance of 60 mm from the nozzle exit.

Thus, the results of computer simulation show that for a proper organisation of the gas-dynamic process of flow mixing and active medium preparation, the small-signal gain can be increased significantly. The quantity K_g is an indirect indicator of the quality of the active medium. Apparently, the energy parameters of the laser must also improve substantially in this case.

3. Experimental studies of the parameters of a COIL with a modernised nozzle bank

The modified design of the nozzle bank (Fig. 11) for a 10-kW COIL [2] was developed using the results of computer simulation of mixing. The nozzle elements are made of a copper alloy and plastic, and the temperature of the nozzles was maintained automatically at a level of 70–80 °C.

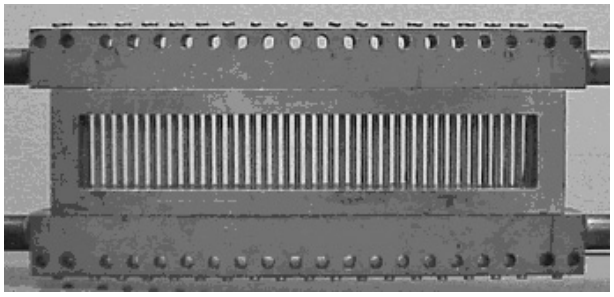

Figure 11. Nozzle bank with a modernised iodine injector.

The experimentally measured value of the small-signal gain averaged along the optical axis of the resonator is 0.5 m^{-1}, which is 1.6 times higher than for the basic configuration [2] (Fig. 12). A stable supersonic flow with a Mach number equal to about 2.3 is established in the resonator (without energy extraction from the flow). In the lasing mode, the value of Mach number increases to 2.4 and a static pressure equal to 1.8 Torr is established.

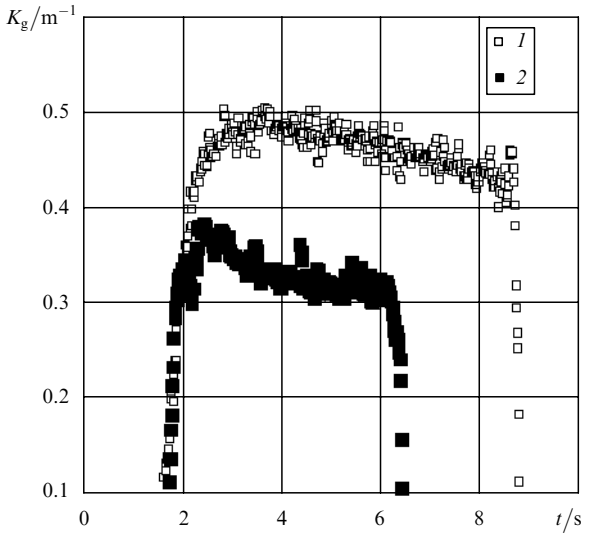

Figure 12. Experimental time dependences of the gain for a modernised iodine injector (*1*) and the injector described in [2] (*2*).

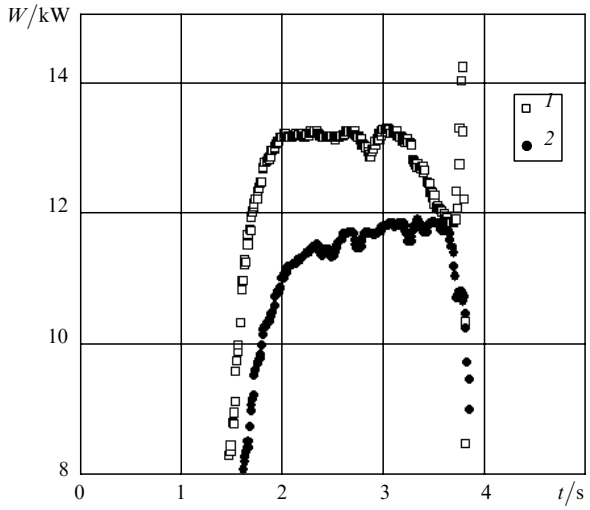

Figure 13. Experimental time dependences of the laser radiation power for a modernised iodine injector (*1*) and the injector described in [2] (*2*).

In experiments on lasing with a stable resonator (the transmission coefficient of the output mirror $\tau = 0.1$), an output power of 13.5 kW was achieved for an iodine flow rate of 10–12 mmole s^{-1} and a chlorine flow rate of 470 mmole s^{-1} (Fig. 13), which corresponds to a chemical efficiency of 31.5 %.

4. Features of the cryosorption systems used for the exhaust of gases from a COIL

The use of cryosorption technique made it possible to solve the problem of exhaust of the discharged active medium of a COIL irrespective of the external pressure. Unlike the traditional application of this technique, the values of the specific flow rate of the adsorbed gas as well as the pressure are quite high under the conditions of operation of laser systems. The microgeometrical parameters of the adsorbent as well as its geometrical structure at all intermediate stages exert a certain influence on the adsorption rate. The method used for supplying the gas being adsorbed with minimum pressure losses and the method of removal of the heat of adsorption are critically important factors. Hence it is expedient to use the empirical dynamic adsorbability α (measured in $m^3\ kg^{-1}\ s^{-1}$) for the main parameter of the adsorbent.

Figure 14 shows the experimental cryoadsorption pump having the form of a hermetically sealed vessel with aluminium heat exchanger and pipeline for liquid nitrogen. The space between the heat exchanger surfaces is filled by the adsorbent (13 kg of NaX type zeolite). Such a construction ensures a low flow resistance for the gas being adsorbed and an effective removal of the released heat of adsorption. Atmospheric air was used as the gas being adsorbed in the experiments.

The pneumo-hydraulic circuit of the cryopump is shown in Fig. 15. The data acquisition system records the time dependence of pressure in the pump cavity at a frequency of 100 Hz. The pump cavity is preliminarily evacuated to a pressure of less than 1 Torr at room temperature. After holding in vacuum for several hours (during which the adsorbent surface is completely purged from gases), liquid nitrogen is supplied to the heat exchanger. The adsorbent

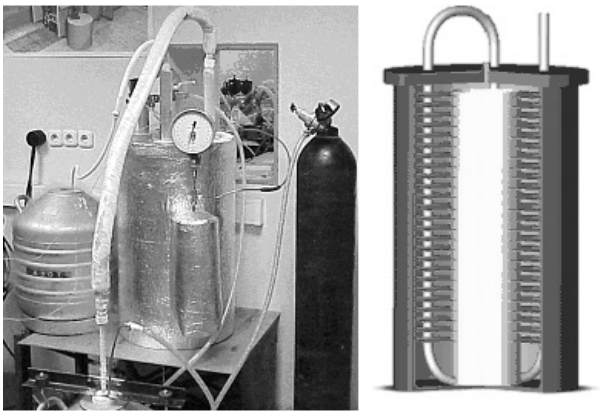

a b

Figure 14. A model cryosorption pump: general view (a) and sectional view (b).

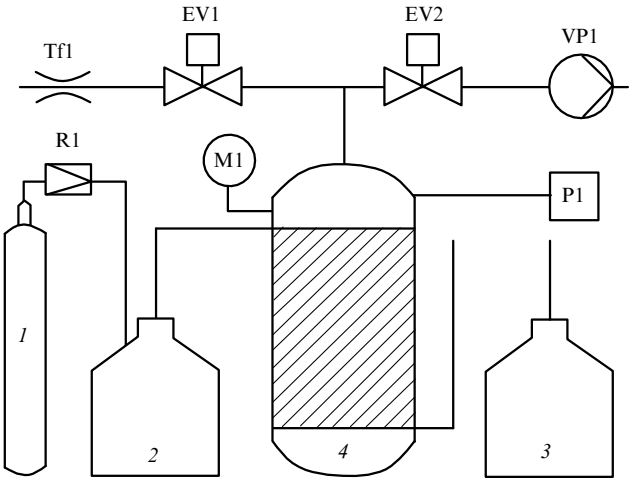

Figure 15. Pneumo-hydraulic circuit of the model cryopump: (*1*) nitrogen gas cylinder; (*2*, *3*) Dewar flasks; (*4*) the cryopump; P1 is the pressure gauge; M1 is the compound pressure and vacuum gauge; R1 is the reducer; EV1, EV2 are the electronic valves; Tf1 is the throttling flow washer; VP1 is the vacuum pump.

temperature is monitored continuously. As soon as it attains a value of about 100 K, the valve EV1 is opened and the atmospheric air enters the pump cavity through the throttling flow nozzle Tf1. Filling of cavity with air is monitored by a control system working in the regime 5 s for let-in with pauses of 5 s.

The dynamic adsorption of the used active medium of the COIL is described by the differential equation

$$\frac{\mathrm{d}p}{\mathrm{d}t} = \frac{RT}{V}\dot{M} - p\frac{\alpha m_\mathrm{c}}{V}, \tag{12}$$

where p is the pressure in the pump cavity; T is the zeolite temperature; V is the pump volume; $\dot{M}$ is the molar flow rate of the gas; $\alpha = C(1-f)(2\pi\mu_\mathrm{g}kT)^{-1/2}$ is the dynamic adsorption coefficient (measured in $\mathrm{m^3\ kg^{-1}\ s^{-1}}$) [10]; C is an empirical factor depending on the microgeometrical characteristics of the adsorbent; f is the saturation factor of the adsorbent surface; μ_g is the molecular mass of the gas being adsorbed; and m_c is the zeolite mass. The first and second terms in Eqn (12) describe isothermal compression and dynamic adsorption, respectively.

The isothermal model can be used for describing the gas state in the cryoadsorption pump cavity only if the rate of heating of the medium as a result of adiabatic compression is much lower than the rate of gas cooling through the transfer of heat to the cold adsorbent. This condition can be described by the expression

$$\frac{\dot{M}}{V} \ll (\gamma - 1)\frac{a_\mathrm{g}}{d_\mathrm{p}^2}\frac{p}{R_0 T}, \tag{13}$$

where the left-hand side contains the specific molar flow rate of the gas per unit volume of the pump cavity; a_g is the thermal diffusivity of the gas; γ is the specific heat ratio; and d_p is the characteristic size of the porous adsorbent structure. According to another important condition, a rapid distribution of the heat of adsorption and the heat of adiabatic compression is required in the bulk of the adsorbent. This prevents an increase in the temperature of the adsorbent surface. This means that

$$\frac{\dot{M}}{V} \ll \frac{c_\mathrm{s}T\rho_\mathrm{s}}{q_\mathrm{a}}\frac{a_\mathrm{s}}{d_\mathrm{p}^2}, \tag{14}$$

where c_s and a_s are the thermal diffusivity and specific heat of the adsorbent; ρ_s is its packed density; and q_a is the heat of adsorption ($\mathrm{J\ mole^{-1}}$). It can be shown that conditions (13) and (14) are satisfied approximately under conditions typical for the COIL exhaust gas system. This allows us to use the isothermal model for describing the state of the gaseous medium in the cryoadsorption pump cavity.

Figure 16 shows the results of the experiment. For a zeolite temperature of 110 K and an air flow rate of 0.23 mole $\mathrm{s^{-1}}$, the pressure growth rate is about 2.5 Torr $\mathrm{s^{-1}}$. Approximation of the experimental data by the solution of Eqn (12) for $f \to 0$ leads to a value 9.8×10^{-3} for the constant C.

The obtained data make it possible to estimate the parameters of the cryosorption pumps for the COIL exhaust. These parameters (especially the adsorbent mass)

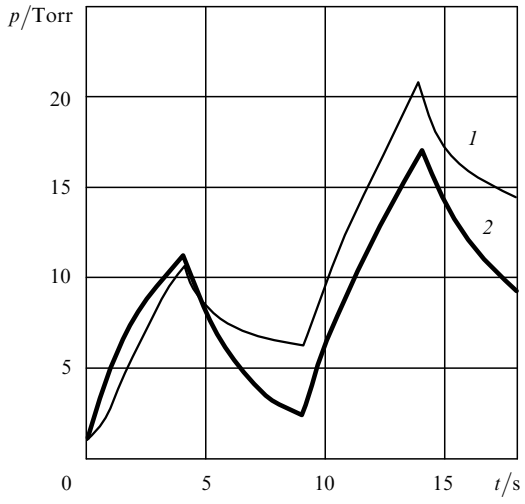

Figure 16. Time dependences of pressure in the cryosorption pump cavity for $M = 0.23$ mole $\mathrm{s^{-1}}$ and $T = 110$ K [curves (*1*) and (*2*) correspond to experiment and theory, respectively].

depend on the recovered pressure of the active medium discharged at the outlet of the supersonic diffuser. The continuous operation of a 10-kW COIL with transsonic iodine injection [2] for 5 s under a maximum recovered pressure of 12 Torr and a total flow rate of about 1.7 mole s^{-1} for the discharged medium requires a cryosorption pump containing about 100 kg of the zeolite NaX at a temperature not exceeding 110 K.

5. Conclusions

We have considered the methods for increasing the efficiency of a COIL [2] containing nitrogen as a buffer gas. A two-layer gas-dynamic model is used for a parametric analysis of physicochemical processes occurring in the transsonic iodine injector and in the COIL cavity, including mixing and generation of radiation. The conditions imposed on the mixing process from the point of view of transformation of chemical energy into the energy of optical radiation are formulated. The 3D-RANS computer simulation software is used to study the flow structures resulting from an injection of iodine-containing flow in the transsonic zone of the oxygen nozzle. The gas-dynamic features of these flows are analysed and the methods for constructing an effective mixing scheme are formulated. Experiments with a 10-kW modified laser have resulted in a chemical efficiency of 31.5 % for a lasing power of 13.5 kW. The results of experimental studies of the cryosorption exhaust system of the 10-kW COIL are presented. The dynamic adsorption ability is measured under the conditions of operation of such lasers.

References

1. Boreysho A.S., Khailov V.M., Mal'kov V.M., Savin A.V. *Proc. SPIE Int. Soc. Opt. Eng.*, **4184**, 401 (2000).
2. Boreisho A.S., Mal'kov V.M., Savin A.V., Vasil'ev D.N., Evdokimov I.M., Trilis A.V., Strakhov S.Yu. *Kvantovaya Elektron.*, **33**, 307 (2003) [*Quantum Electron.*, **33**, 307 (2003)].
3. Savin A.V. *Proc. SPIE Int. Soc. Opt. Eng.*, **5547**, 39 (2004).
4. Savin A.V., Ignatiev A.A., Fedotov A.V. *Proc. SPIE Int. Soc. Opt. Eng.*, **4184**, 410 (2000).
5. Barmashenko B.D., Elior A., Lebiush E., Rosenwaks S.J. *Appl. Phys.*, **75** (12), 7653 (1994).
6. Abramovich G.N. *Prikladnaya gazovaya dinamika* (Applied Gas Dynamics) (Moscow: Nauka, 1991).
7. Lapin Yu.V. *Pogranichniy sloi v giperzvukovykh potokakh* (Boundary Layer in Hypersonic flows) (Moscow: Nauka, 1976).
8. Madden T.J. *Proc. SPIE Int. Soc. Opt. Eng.*, **5120**, 363 (2002).
9. Zlobin V. *Izv. Akad. Nauk Eston. SSR*, **20**, 66 (1971).
10. Hefer R. *Kriovakuumnaya tekhnika* (Cryovacuum Technology) (Moscow: Energoatomizdat, 1983).